

CONTROL OF VIBRATION USING SURFACE MOUNTED ACOUSTIC BLACK HOLES

Joe Tan^{1*} Jordan Cheer¹

¹ ISVR, University of Southampton, United Kingdom

ABSTRACT

Acoustic Black Holes (ABHs) are tapered features that can either be surface mounted or embedded into structures to provide effective broadband structural damping. Generally, structures with embedded ABHs require material to be removed from the structure to create the required geometric features. However, for thin plates, it is not straightforward to embed ABHs, since the removal of the material in this case will significantly impact the strength of the structure. Therefore, this paper presents a numerical model based investigation into how surface mounted ABHs can be used to control the vibration of a thin beam over a broad frequency range. The numerical investigation compares the performance of the proposed surface mounted ABHs with a beam treated using conventional passive measures via evaluation of the total kinetic energy of the primary structure. The results presented in this paper show that the surface mounted ABHs achieve greater total kinetic energy attenuation compared to the conventionally treated beam over the presented bandwidth due to the ABH effect. The proposed surface mounted ABHs could be used as an effective broadband vibration control solution for thin structures, where it is not straightforward to design effective embedded ABHs.

Keywords: *acoustic black holes, vibration control, dynamic vibration absorber*

*Corresponding author: j.tan@soton.ac.uk.

Copyright: ©2023 J.Tan and J.Cheer This is an open-access article distributed under the terms of the Creative Commons Attribution 3.0 Unported License, which permits unrestricted use, distribution, and reproduction in any medium, provided the original author and source are credited.

1. INTRODUCTION

ABHs have the ability to provide effective broadband structural damping for beams and plates via tapered geometrical features, where the thickness of the structure is smoothly decreased. For one-dimensional beams, the flexural wave speed is related to the thickness profile of the ABH taper, such that the phase velocity gradually reduces as the wave propagates along the taper, which leads to low reflection from the tip. In practice, the taper requires a small amount of damping material to achieve good passive performance and it has been shown that the location of the damping material can be optimised to minimise the vibration [1–3] or radiated sound [4, 5]. For plates, the thickness profile of the ABH can smoothly vary in the radial direction to create a type of lens, which focuses the flexural wave energy to the thinnest part of the ABH. Similarly to the beam case, a small amount of damping material can also be applied to the ABH to dissipate the flexural wave energy. ABHs in this case have been realised through surface-mounted vibration dampers [6, 7] or embedded tapered features [8–13], where material is typically removed from the host structure to create the desired taper. It has been shown that the ABH effect can be used in a wide range of applications, for example, vibration and noise control and energy harvesting [14, 15].

Although embedded ABHs can achieve good damping performance, they require the removal of material from the host structure, which can affect the stiffness and strength of the host structure. In terms of thin plates, it may not be straightforward to design an effective embedded ABH without significantly reducing the structural integrity of the host structure. To address this limitation, this paper presents a simulation-based investigation into how a surface-mounted ABH can be used to control the vibration

of a thin two-dimensional cantilever beam. Although previous surface-mounted ABHs have been proposed [6, 7], these devices were still used to control vibration of thick beams and plates. The proposed surface-mounted ABH aims to control the vibration of the thin beam over a large bandwidth, whilst the mass of the add-on device is significantly lower than the mass of the host structure.

This paper is structured as follows: Section 2 describes the proposed surface-mounted ABH and the three different beam configurations used to assess the performance of the proposed surface-mounted ABH. Section 3 presents the results of the numerical simulations and Section 4 presents the conclusions.

2. THE SURFACE-MOUNTED ABH AND BEAM CONFIGURATIONS

This section describes the proposed surface-mounted ABH and the three different beam configurations used to assess the performance of the proposed ABH: a cantilever beam with no passive treatment, the cantilever beam with the proposed surface-mounted ABH and the cantilever beam with an equivalent damped mass attached.

The surface-mounted ABH used in this paper is shown in Figure 1. This add-on device consists of a primary taper, which is defined by a power-law height profile and it can be calculated as

$$h(r) = \varepsilon \left(\frac{r}{r_{inner}} \right)^\mu + h_{min} \quad (1)$$

where $\varepsilon = h_{min} - h_{abh}$ is a scaling factor, $h_{min} = h_{abh} - h_0$ is the minimum height of the ABH, h_0 is the difference between the overall height of the ABH and minimum height, μ is the power law used to define the gradient of the taper and r_{inner} is the radius of the ABH. A thin layer of damping material is applied to the minimum height region of the ABH as shown in Figure 1. The geometric parameters of the ABH shown in Figure 1 are presented in Table 1. These geometric parameters were selected to be consistent with existing embedded ABHs, for example [13]. The geometric parameters presented in Table 1 are not the optimal set of geometric parameters for the proposed ABH, however, they can provide an initial case to assess the performance of the proposed ABH. To evaluate the performance of the proposed ABH, this paper compares kinetic energy for the three different beam configurations stated earlier in this section and the kinetic energy has been calculated via numerical simulations.

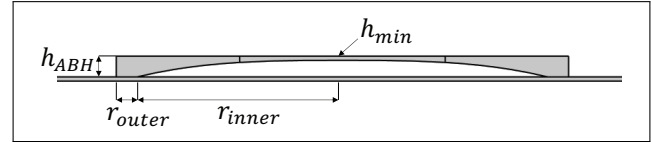


Figure 1. The proposed surface-mounted ABH.

The numerical models of the three different beam configurations have been developed in COMSOL MultiPhysics® using a 2D solid mechanics model in the frequency domain and these numerical models are shown in Figure 2. The ABH shown in Figure 1 and the beam shown in Figure 2 were assumed to be constructed from aluminium and the inherent damping within this material was included via an isotropic loss factor of $\eta_{beam} = 0.0001$, which is consistent with previous literature [12, 16, 17]. The damping layer within the minimum thickness region of the ABH has been modelled using an isotropic loss factor of $\eta_{ABH} = 0.2$ and an evenly distributed mass of 9.4g has been applied to this region of the ABH to represent the mass of the damping. This method for modelling the damping layer is consistent with previous literature and it has been shown to provide a good approximation of the behaviour of the damping layer. The dimensions of the beam and damped mass shown in Figure 2 are also presented in Table 1.

Table 1. The geometrical parameters used to design the proposed surface-mounted ABH.

Parameter	Symbol	Value
Inner Taper Radius	r_{inner}	70 mm
Minimum height of the ABH	h_{min}	0.5 mm
Overall height of the ABH	h_{abh}	1.5 mm
Attachment Point radius	r_{outer}	5 mm
Inner Taper Power Law	μ	4
Beam width	w	0.2 m
Beam length	l	0.5 m
Beam height	h	1 mm
Radius of the damped mass	r_{mass}	75mm
Damped mass height	h_{mass}	1.5mm

In order to compare the performance of the damped mass and ABH, both of these devices need to have the

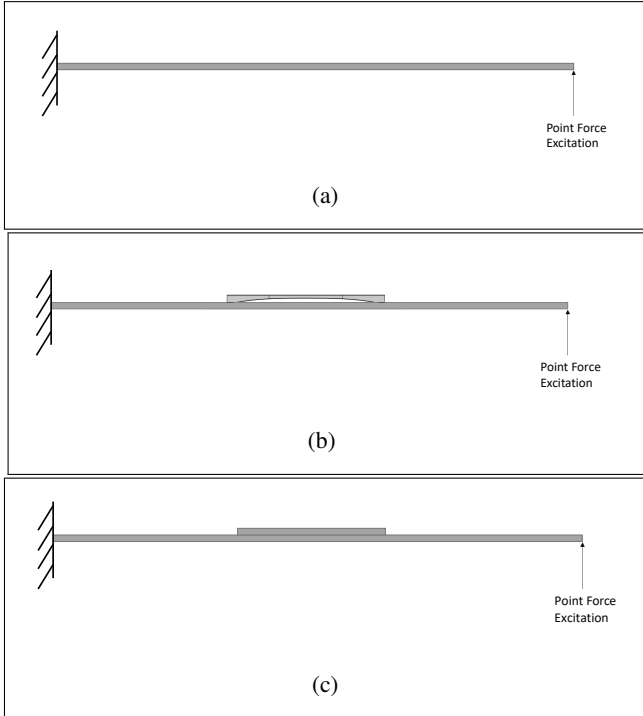


Figure 2. The three different numerical models used to evaluate the performance of the proposed surface-mounted ABH: a cantilever beam (a), a cantilever beam with a surface-mounted ABH attached at the centre (b) and a cantilever beam with a damped mass attached at the centre.

same area of damping. This has been achieved by scaling the isotropic loss factor of the damped mass by the ratio between the damped ABH region, A_{ABH} , and the damped mass, A_{mass} areas, which can be calculated as

$$\eta_{mass} = \eta_{ABH} \frac{A_{ABH}}{A_{mass}}. \quad (2)$$

Using Eq. 2, the isotropic loss factor for the damped mass in this case is $\eta_{mass} = 0.033$.

In each beam configuration, the initial conditions have been set to stationary and a fixed boundary condition has been applied to one end of the beam and a vertical point excitation force has been applied on the opposite end as shown in Figure 2. To ensure that each numerical model has sufficient accuracy, a mesh convergence study has been conducted at the upper frequency limit for each configuration. When fully converged, the number of elements for the beam, proposed ABH and damped mass models are

723, 1078 and 1115 respectively. Using the three numerical models described in this section, the kinetic energy for each configuration has been calculated directly from each numerical model over the frequency range 10 Hz to 10 kHz, in steps of 2 Hz, and these results are presented in the next section.

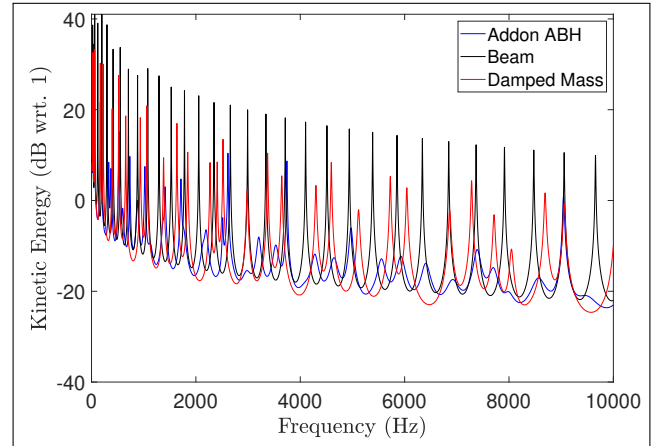


Figure 3. The frequency response of the kinetic energy for the three beam configurations: an untreated cantilever beam (black line), a cantilever beam with a damped mass attached (red line) and a cantilever beam with the proposed ABH attached (blue line).

3. RESULTS

The kinetic energy has been calculated directly from the three beam numerical models described in Section 2 over the frequency range of interest and these results are presented in Figure 3. The black, red and blue lines in Figure 3 show the frequency response of the untreated cantilever beam, the beam with the damped mass attached and the beam with the proposed ABH attached respectively. From Figure 3, it can be seen that the untreated cantilever beam and damped mass cases have clear resonant peaks in the kinetic energy response, however, the resonant peaks in the damped mass treated case are lower in magnitude compared to the untreated case and the additional mass and stiffness of the damped mass on the system has shifted the location of the resonant peaks. In the case of the surface-mounted ABH, Figure 3 shows that the addon device achieves a higher level of attenuation in the resonant peaks compared to the damped mass case at the majority of the resonances above 500 Hz. Since the damped mass

and proposed ABH both have the same dimensions, material and area of damping, this suggests that the higher level of broadband damping achieved by the proposed ABH is due to the ABH effect, although it could also be related to the differences in the contact regions of the two devices and the resulting coupling to the beam. Below 500 Hz, the proposed ABH achieves a similar level of attenuation to the damped mass case because the ABH does not absorb the incident waves, since the incident wavelength is much larger than the ABH taper length at these frequencies and this frequency is defined as the cut-on frequency of the ABH. It can be seen in Figure 3 that the proposed ABH achieves a similar level of attenuation to the damped mass at three resonant peaks above the cut-on frequency of the ABH because this ABH does not have sufficient coupling to the beam and, therefore, the incident waves at these frequencies do not enter the ABH. There are two main reasons for the decoupling between the beam and the ABH at these frequencies: the positioning of the ABH on the beam and the mode shapes of both the ABH and the beam. Despite the decoupling between beam and plate at certain frequencies, the results presented in Figure 3 show that the proposed ABH achieves significant effective damping over the presented bandwidth. The broadband average kinetic energy attenuation has also been calculated for both the surface-mounted ABH and damped mass configurations, where the surface-mounted ABH and damped mass configurations achieve 3 dB and 1 dB respectively. The broadband average kinetic energy attenuation and the results presented in Figure 3 show that the proposed surface-mounted ABH provides more effective broadband damping compared to the damped mass configuration.

4. CONCLUSIONS

ABHs are structural features that can achieve broadband effective damping in beams and plates. These structural features are typically combined with the host structure by either surface-mounting or through embedding into the host structure. Although surface-mounted ABHs have been previously proposed [6, 7], these devices were still implemented on thick beams and plates.

This paper presents a simulation-based investigation into how a surface-mounted ABH can be used to control the vibration of a thin cantilever beam. The performance of the ABH has been assessed by comparing the frequency response of the kinetic energy for three beam configurations: an untreated cantilever beam, a beam with an equivalent damped mass attached and a beam with the

proposed ABH attached. Although the geometric parameters of the ABH have not been optimised, the simulation results presented in this paper have shown that the surface-mounted ABH achieves significantly more damping compared to the equivalent damped mass case over the cut-on frequency of the ABH. The advantage of the proposed surface-mounted ABH is that this device could be retrofitted to existing thin structures, which enables ABHs to be used in a wider range of applications.

5. ACKNOWLEDGMENTS

This research was supported by the Intelligent Structures for Low Noise Environments EPSRC Prosperity Partnership (EP/S03661X/1).

6. REFERENCES

- [1] M. R. Shepherd, C. A. McCormick, S. C. Conlon, and P. A. Feurtado, "Modeling and optimization of acoustic black hole vibration absorbers," *The Journal of the Acoustical Society of America*, vol. 141, no. 5, pp. 4034–4034, 2017.
- [2] C. A. McCormick and M. R. Shepherd, "Design optimization and performance comparison of three styles of one-dimensional acoustic black hole vibration absorbers," *Journal of Sound and Vibration*, vol. 470, p. 115164, 2020.
- [3] L. Ma, H.-W. Dong, and L. Cheng, "An alternative and optimized thickness profile of an acoustic black hole plate," *Journal of Sound and Vibration*, vol. 486, p. 115619, 2020.
- [4] E. Bowyer and V. V. Krylov, "Experimental study of sound radiation by plates containing circular indentations of power-law profile," *Applied Acoustics*, vol. 88, pp. 30–37, 2015.
- [5] E. P. Bowyer and V. V. Krylov, "A review of experimental investigations into the acoustic black hole effect and its applications for reduction of flexural vibrations and structure-borne sound," 2015.
- [6] T. Zhou and L. Cheng, "A resonant beam damper tailored with acoustic black hole features for broadband vibration reduction," *Journal of Sound and Vibration*, vol. 430, pp. 174–184, 2018.

- [7] H. Ji, N. Wang, C. Zhang, X. Wang, L. Cheng, and J. Qiu, "A vibration absorber based on two-dimensional acoustic black holes," *Journal of Sound and Vibration*, vol. 500, p. 116024, 2021.
- [8] O. Unruh, C. Blech, and H. P. Monner, "Numerical and experimental study of sound power reduction performance of acoustic black holes in rectangular plates," *SAE International Journal of Passenger Cars-Mechanical Systems*, vol. 8, no. 2015-01-2270, pp. 956–963, 2015.
- [9] L. Ma and L. Cheng, "Topological optimization of damping layout for minimized sound radiation of an acoustic black hole plate," *Journal of Sound and Vibration*, vol. 458, pp. 349–364, 2019.
- [10] X. Liu, J. Yuan, H. Liang, and Z. Wang, "Study on energy propagation and noise radiation in plates containing the array of acoustic black holes," in *INTER-NOISE and NOISE-CON Congress and Conference Proceedings*, vol. 261, pp. 5245–5254, Institute of Noise Control Engineering, 2020.
- [11] H. Ji, X. Wang, J. Qiu, L. Cheng, Y. Wu, and C. Zhang, "Noise reduction inside a cavity coupled to a flexible plate with embedded 2-d acoustic black holes," *Journal of Sound and Vibration*, vol. 455, pp. 324–338, 2019.
- [12] P. A. Feurtado and S. C. Conlon, "An experimental investigation of acoustic black hole dynamics at low, mid, and high frequencies," *Journal of Vibration and Acoustics*, vol. 138, no. 6, 2016.
- [13] K. Hook, J. Cheer, and S. Daley, "A parametric study of an acoustic black hole on a beam," *The Journal of the Acoustical Society of America*, vol. 145, no. 6, pp. 3488–3498, 2019.
- [14] L. Zhao, S. C. Conlon, and F. Semperlotti, "Broadband energy harvesting using acoustic black hole structural tailoring," *Smart materials and structures*, vol. 23, no. 6, p. 065021, 2014.
- [15] L. Zhao, S. C. Conlon, and F. Semperlotti, "An experimental study of vibration based energy harvesting in dynamically tailored structures with embedded acoustic black holes," *Smart Materials and Structures*, vol. 24, no. 6, p. 065039, 2015.
- [16] C. McCormick and M. Shepherd, "Optimal design and position of an embedded one-dimensional acoustic black hole," in *INTER-NOISE and NOISE-CON Congress and Conference Proceedings*, vol. 258, pp. 1345–1354, Institute of Noise Control Engineering, 2018.
- [17] S. C. Conlon, J. B. Fahnlone, and F. Semperlotti, "Numerical analysis of the vibroacoustic properties of plates with embedded grids of acoustic black holes," *The Journal of the Acoustical Society of America*, vol. 137, no. 1, pp. 447–457, 2015.